J. Fluid Mech. (2019), *vol.* 860, *pp.* 822–836. © Cambridge University Press 2018
doi:10.1017/jfm.2018.897

Viscosity, surface tension and gravity effects on acoustic reflection and refraction

R. Krechetnikov†

Department of Mathematics, University of Alberta, Edmonton, AB, T6G 2G1, Canada

(Received 9 August 2018; revised 7 October 2018; accepted 4 November 2018;
first published online 14 December 2018)

The idea of the present work is to study from a unifying viewpoint the effects of viscosity, surface tension and gravity on acoustic reflection and refraction at a fluid interface, with the focus on modifications of Snell's (Snell–Descartes') law. While all these effects can be treated individually due to separation of the associated time scales, the contributions of surface tension to the gravity and viscosity cases are considered as well. The analysis reveals a number of phenomena among which are dispersive refraction laws, surface tension enhancing reflection, acoustic field generating vorticity at the interface, and viscosity enhancing/suppressing reflection as well as giving rise to extra reflected and transmitted waves.

Key words: acoustics, interfacial flows (free surface)

1. Introduction

Given a sound wave propagating in a medium with speed c, its wavelength $\lambda = 2\pi c/\omega$ is set by the frequency ω, which is treated as a fixed parameter here: we consider the physical situation of an acoustic source generating a plane wave of frequency ω. From dimensional analysis, it follows that the presence of gravity sets up three frequencies: $\omega_g = g/c$ due to acceleration g, and $\omega_g' = \sqrt{g|\dot{\rho}|/\rho}$ and $\omega_g'' = c\sqrt{|\ddot{\rho}|/\rho}$ due to density stratification ($\dot{\rho}$ and $\ddot{\rho}$ are the first and second derivatives of the density ρ with respect to the stratification coordinate). The frequency ω_g' is related to buoyancy as encountered in the internal gravity wave theory (though it will prove to be irrelevant for our purposes). Similarly, the surface tension σ between fluids leads to the frequency $\omega_\sigma = \rho c^3/\sigma$, and the viscosity ν of the medium sets yet another one $\omega_\nu = c^2/\nu$. Typically, these frequencies range from infrasound to ultrasound: $\omega_g \ll \omega_\sigma \ll \omega_\nu$, with ω_g disparate from ω_g' and ω_g''. Examples of infrasound include (Whitaker & Norris 2008) signals from animals (whales, elephants and giraffes), avalanches, volcanoes, earthquakes, ocean waves, waterfalls and meteors, nuclear and chemical explosions, engines, machinery and airplanes, which can be detected at enormous distances due to very little attenuation. Moreover, in the ocean there exists a horizontal layer of water – a sound fixing and ranging also known as a deep sound channel – which acts as a waveguide for low-frequency sound waves converging to it from a variety of sources (e.g. underwater landslides, earthquakes, explosions) due to density stratification and travelling thousands of miles before attenuating

† Email address for correspondence: krechet@ualberta.ca

https://doi.org/10.1017/jfm.2018.897 Published online by Cambridge University Press

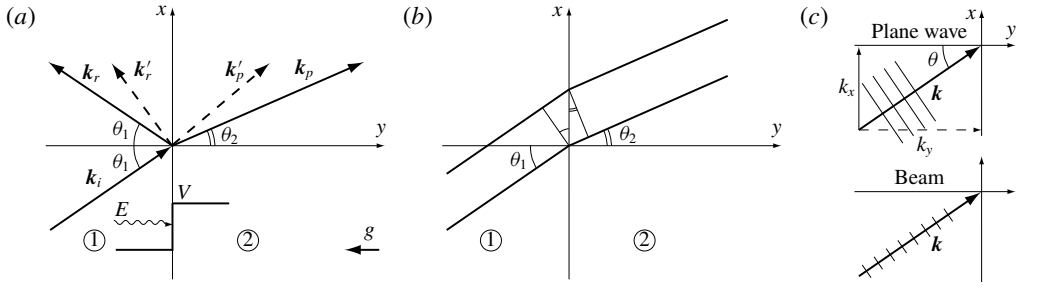


FIGURE 1. (*a*) Setting: incident (*i*), reflected (*r*) and refracted (*p*) waves. (*b*) The change of an acoustic beam cross-section $\mathcal{A}$: $\mathcal{A}_i/\mathcal{A}_p = \cos\theta_1/\cos\theta_2$. (*c*) Two types of sound waves: plane and a narrow beam (a ray).

(Munk *et al.* 1994). On the other hand, the viscosity and surface tension lead to ultrasonic frequencies, which become important in modern applications, including therapeutics up to 3 MHz (Watson & Young 2008), probing the underwater environment up to 10 MHz (Dahl 2007), lab-on-a-chip surface acoustic waves and microparticle manipulations up to 200 MHz (Drinkwater 2016), and acoustic microscopy and sonography up to 4 GHz (Papadakis 1999). Viscous effects also come into play in the geophysical context, again in the propagation and dissipation of low-frequency hydro-acoustic waves in an ocean overlying a weakly compressible viscous sediment layer (Abdolali, Kirby & Bellotti 2015). Naturally, in all the above-mentioned situations, acoustic reflection and refraction from fluid interfaces become important.

In the classical case of media with different densities ρ and sound speeds c (cf. figure 1*a*), the solutions to the wave equations in each medium for the velocity potential ϕ defined via $\nabla\phi = \boldsymbol{v}$,

$$\phi^n_{tt} - c_n^2[\phi^n_{xx} + \phi^n_{yy}] = 0, \quad \text{for } x \in \mathbb{R},\ \ y \in (-1)^n\mathbb{R}^+,\ \ n = 1, 2, \tag{1.1}$$

satisfy the kinematic and dynamic conditions at the interface, linearized about its undisturbed position and with the notation $[\cdots]_1^2$ for the jump of a quantity between two media represented as

$$y = 0\text{:}\quad [\phi_y]_1^2 = 0, \quad [p]_1^2 = -[\rho\phi_t]_1^2 = 0, \tag{1.2a,b}$$

accounting for the continuity (across the interface) of the vertical velocity component $v = \phi_y$ and the pressure p, respectively. Representing the incident, reflected and transmitted waves as $\phi_i^1 = A_i e^{i\psi_i}$, $\phi_r^1 = A_r e^{i\psi_r}$ and $\phi_p^2 = A_p e^{i\psi_p}$, correspondingly, with $\psi_m = \boldsymbol{k}_m \cdot \boldsymbol{x} - \omega_m t$ (entailing that $\boldsymbol{v} \equiv (u, v)$ is parallel to $\boldsymbol{k}$), where we have kept the frequencies ω_m and wavenumbers $\boldsymbol{k}_m = (k_x^m, k_y^m)$ independent, from (1.1) we find the corresponding dispersion relations:

$$\omega_i^2 = c_1^2|\boldsymbol{k}_i|^2, \quad \omega_r^2 = c_1^2|\boldsymbol{k}_r|^2, \quad \omega_p^2 = c_2^2|\boldsymbol{k}_p|^2. \tag{1.3a–c}$$

Substituting the velocity potentials into the boundary conditions (1.2) we conclude that the only way for the latter to hold is if $k_x^i = k_x^r = k_x^p \equiv k_x$ and $\omega_i = \omega_r = \omega_p \equiv \omega$, i.e. the x-component of the wavenumber remains unchanged and all three waves oscillate at the same frequency ω.

https://doi.org/10.1017/jfm.2018.897 Published online by Cambridge University Press

With these observations and the linear independence of the harmonics, equations (1.2) reduce to an algebraic system, i.e. $k_y^i A_i + k_y^r A_r = k_y^p A_p$ and $\rho_1(A_i + A_r) = \rho_2 A_p$, the solution of which is

$$\Gamma \equiv \frac{A_r}{A_i} = \frac{\rho_2 k_y - \rho_1 \kappa_y}{\rho_2 k_y + \rho_1 \kappa_y} \left(= \frac{\widehat{u}_r}{\widehat{u}_i} \right), \quad \frac{A_p}{A_i} = \frac{2\rho_1 k_y}{\rho_2 k_y + \rho_1 \kappa_y}. \tag{1.4a,b}$$

Here the y-components of $\boldsymbol{k}_m$ are determined from (1.3), i.e. $k_y^{m2} = \omega_m^2 - k_x^{m2}$ and

$$-k_y^r = k_y^i \equiv k_y = k_x/\tan\theta_1, \quad k_y^p \equiv \kappa_y = k_x/\tan\theta_2, \tag{1.5a,b}$$

after we have used the above established facts that k_x and ω are the same in both media. From the equality $k_y^r = -k_y^i$ it follows that the angle of incidence is equal to the angle of reflection, $\theta_i = \theta_r \equiv \theta_1$, measured with respect to the normal to the boundary (cf. figure 1*a*). With further geometric considerations we arrive at Snell's (also known as Snell–Descartes') law of refraction relating angles θ_1 and θ_2:

$$\frac{k_x^i}{k_x^p} = 1 = \frac{|\boldsymbol{k}_i|}{|\boldsymbol{k}_p|}\frac{\sin\theta_1}{\sin\theta_2} = \frac{\omega/c_1}{\omega/c_2}\frac{\sin\theta_1}{\sin\theta_2} \quad \Rightarrow \quad \frac{\sin\theta_1}{\sin\theta_2} = \frac{c_1}{c_2}, \tag{1.6}$$

with well-known properties (Kinsler *et al.* 1999). As follows from (1.4a), (1.5) and (1.6), for $\theta_1 > \theta_c$, where the critical angle θ_c is found from $\sin\theta_1 = c_1/c_2$ for $c_1 < c_2$, κ_y becomes imaginary and hence the transmitted wave evanescent (though the transmitted wave energy is still non-zero), so that the Rayleigh reflection coefficient Γ in (1.4*a*) is no longer real. In fact, Γ has complex conjugate numerator and denominator, meaning that its amplitude $|\Gamma| = 1$ corresponds to total reflection, but since Γ is complex there is a phase shift between the incident and reflected waves.

The energy conservation states that the averaged $\langle\cdot\rangle$ energy flux density $\boldsymbol{q} = p'\boldsymbol{v} = \rho c|\boldsymbol{v}|^2\boldsymbol{n}$ over the period $2\pi/\omega$ (here $\boldsymbol{n} = \boldsymbol{k}/k$ and p' is the pressure of the acoustic wave) in the reflected and transmitted waves should add up to that of the incident wave, $\langle\mathcal{R}_0\rangle + \langle\mathcal{T}_0\rangle = 1$, where the reflection and transmission coefficients are $\langle\mathcal{R}_0\rangle = \langle\boldsymbol{q}_r\cdot\boldsymbol{n}_r\rangle/\langle\boldsymbol{q}_i\cdot\boldsymbol{n}_i\rangle$ and $\langle\mathcal{T}_0\rangle = (\mathcal{A}_p/\mathcal{A}_i)\langle\boldsymbol{q}_r\cdot\boldsymbol{n}_r\rangle/\langle\boldsymbol{q}_i\cdot\boldsymbol{n}_i\rangle$, respectively. Here we have taken into account the change in the beam cross-section between the transmitted $\mathcal{A}_p$ and incident $\mathcal{A}_i$ waves (with no change between incident and reflected waves); cf. figure 1(*b*). When $\theta_1 > \theta_c$, $\langle\mathcal{R}_0\rangle = 1$, but the instantaneous $\mathcal{R}_0$ is different from unity and, in fact, depends on ω. The sum of the instantaneous incident and reflected energy fluxes is non-zero, thus explaining the penetration of the acoustic signal into medium 2. The existence of the critical angle θ_c can be understood by rewriting (1.1) with $\phi^n(t, x, y) = \Phi^n(y)\mathrm{e}^{\mathrm{i}(k_x x - \omega t)}$, leading to the stationary one-dimensional (1D) Schrödinger equation $\Phi^n_{yy} + (\omega^2/c_n^2 - k_x^2)\Phi^n = 0$, where the expression in brackets has the meaning of the difference between the phonon energy E and potential barrier size V (cf. figure 1*a*): $E - V \sim \omega^2/c_n^2 - k_x^2$ with $V \sim \omega^2(1/c_1^2 - 1/c_2^2) = [\omega^2/c^2]_2^1$. For $c_2 > c_1$ and $\theta_1 > \theta_c$, the energy of the incident phonon is below V and hence it totally reflects from the interface.

2. Surface tension effects

Proceeding in the order of increasing complexity, we first account for surface (interfacial) tension σ between two fluids. The wave equations (1.1) and hence the dispersion relation for sound propagation (1.3) stay intact as surface tension affects only the boundary conditions: (1.2*a*) is appended with $h_t = \phi_y$ and (1.2*b*) generalizes

https://doi.org/10.1017/jfm.2018.897 Published online by Cambridge University Press

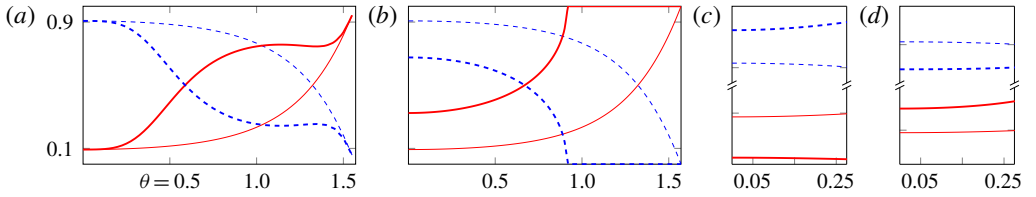


FIGURE 2. (Colour online) (*a*) Surface tension case: $\omega/\omega_\sigma^{(1)} = 5$. (*b*) Gravity case: $\omega/\omega_g^{(2)} = 0.55$. (*c*,*d*) Viscous cases: $\omega/\omega_\nu^{(2)} = 1.0$, $\sigma = 0$, with $\mu_1/\mu_2 = 0.5$ (*c*) and 3.5 (*d*). In all plots $c_1/c_2 = 1.5$ and $\rho_1/\rho_2 = 1.25$. Ticks and lower/upper limits of the ordinate are the same in (*a–d*). Solid lines correspond to $\langle\mathcal{R}\rangle$ and dashed to $\langle\mathcal{T}\rangle$, while thin ones to the classical $\langle\mathcal{R}_0\rangle$ and $\langle\mathcal{T}_0\rangle$.

to $[\rho\phi_t]_1^2 = -\sigma h_{xx}$. With the argument of § 1 and with an extra harmonic representation for the interfacial perturbation $h = A_h e^{i(k_x^h x - \omega_h t)}$, we get three equations for unknown amplitudes A_r, A_p and A_h with the resulting solutions:

$$\{A_r, A_p, A_h\}/A_i = \Delta^{-1}\{\rho_2 k_y - \rho_1\kappa_y + i\sigma k_x^2 k_y k_y/\omega^2,\ \ 2\rho_1 k_y,\ \ -2\rho_1 k_y\kappa_y/\omega\}, \tag{2.1}$$

where $\Delta = \rho_2 k_y + \rho_1\kappa_y + i\sigma k_x^2\kappa_y k_y/\omega^2$ with the notation from (1.5). Notably, the amplitude of the interfacial wave A_h does not vanish with σ, which is due to the kinematic condition. The energy balance $\langle\mathcal{R}\rangle + \langle\mathcal{T}\rangle = 1$ stays intact, i.e. in the steady state the surface waves do not withdraw energy from the incident wave due to the conservative nature of surface tension.

The complexity of the amplitudes, in particular A_r, implies that there is a phase φ associated with it so that the corresponding reflected wave behaves as $\phi_r^1 \sim e^{i(\psi_r+\varphi)}$, i.e. the phase constant φ tells us how much a signal is shifted in time and how efficiently energy is transferred from the driver (incident wave) to the oscillator system (reflected wave). Exploiting a simple relation between time averaging and multiplication of complex amplitudes,

$$\langle(Ae^+ + A^*e^-)(Be^+ + B^*e^-)\rangle = 2(A_rB_r + A_iB_i), \tag{2.2}$$

e.g. when $B \equiv A$, $\langle(Ae^+ + A^*e^-)^2\rangle = 2|A|^2$, in the case of regular reflection, $\theta_1 < \theta_c$, we find

$$\langle\mathcal{R}\rangle = \frac{(k_y\rho_2 - \kappa_y\rho_1)^2 + \sigma^2 k_y^2\kappa_y^2 k_x^4/\omega^4}{(k_y\rho_2 + \kappa_y\rho_1)^2 + \sigma^2 k_y^2\kappa_y^2 k_x^4/\omega^4}, \quad \tan\varphi = \frac{2\sigma\rho_1 k_y\kappa_y^2 k_x^2/\omega^2}{k_y^2\rho_2^2 - \kappa_y^2\rho_1^2 + \sigma^2 k_y^2\kappa_y^2 k_x^4/\omega^4}, \tag{2.3a,b}$$

where $\varphi = \arg\Gamma$. The latter expression (for φ) suggests that surface tension can be responsible for both leading and lagging effects depending on the sign of the denominator in the argument of $\tan^{-1}$. As follows from (2.3), the reflection phenomena are characterized by three non-dimensional parameters, i.e. ρ_1/ρ_2, c_1/c_2 and $\omega/\omega_\sigma^{(1)}$ with $\omega_\sigma^{(1)} = c_1^3\rho_1/\sigma$ evaluated in medium 1, and for particular values are illustrated in figure 2(*a*) exhibiting significant departures from the classical case when $\omega \sim \omega_\sigma$. The value of $\langle\mathcal{R}\rangle$ is closer to unity than that of $\langle\mathcal{R}_0\rangle$ and, in fact, the reflection becomes stronger with increasing frequency ω, meaning that surface tension 'rigidifies' the interface, leading to enhanced reflection. While, as is obvious from (2.3), perfect

https://doi.org/10.1017/jfm.2018.897 Published online by Cambridge University Press

refraction is no longer possible in the presence of surface tension, one can still find a minimum of reflection

$$\langle\mathcal{R}\rangle_{min}=\frac{\sigma^2(c_1^2-c_2^2)k_x^6}{\sigma^2k_x^4(c_1^2-c_2^2)-4\omega^4(c_1^2\rho_1^2-c_2^2\rho_2^2)}, \tag{2.4}$$

which occurs at the classical Brewster angle $\sin^2\theta_B=[1-(\rho_1c_1/\rho_2c_2)^2]/[1-(\rho_1/\rho_2)^2]$. In the case of total reflection, i.e. when $\theta_1>\theta_c$ with $\sin\theta_c=c_1/c_2$, the averaging gives $\langle\mathcal{R}\rangle=1$.

3. Gravity effects

Starting from the Euler system for compressible flow in the gravity field $\boldsymbol{g}$ and superimposing small perturbations of density ρ' and pressure p' on the hydrostatic base state (ρ_0,p_0) governed by $p_0=\int\rho_0\boldsymbol{g}\cdot\mathrm{d}\boldsymbol{x}$, the linearized system for perturbation reads

$$\frac{\partial\rho'}{\partial t}+\rho_0\boldsymbol{\nabla}\cdot\boldsymbol{v}+\boldsymbol{\nabla}\rho_0\cdot\boldsymbol{v}=0,\quad \frac{\partial\boldsymbol{v}}{\partial t}=-\frac{1}{\rho_0}\boldsymbol{\nabla}p'+\boldsymbol{g}\frac{\rho'}{\rho_0}, \tag{3.1a,b}$$

where the last term in (3.1*a*) comes from the base state density stratification and the last term in (3.1*b*) has the meaning of buoyancy. The perturbation for pressure p' is found from

$$p=p_0+p'=p_0+(\partial p/\partial\rho)_{s,\rho_0}\rho'+\cdots\quad\Rightarrow\quad p'=(\partial p/\partial\rho)_{s,\rho_0}\rho'=c_0^2\rho', \tag{3.2}$$

after using the adiabatic assumption (constant entropy s) for sound wave propagation, to be revisited in § 4. The corresponding interfacial conditions are again the kinematic and dynamic

$$y=0:\quad h_t=v^1=v^2,\quad [p']_1^2=[c_0^2\rho']_1^2=\sigma h_{xx}\quad\Rightarrow\quad [c_0^2\rho_t']_1^2=\sigma h_{txx}, \tag{3.3a,b}$$

where in the latter condition we exploited (3.2) and differentiated with respect to time as our goal is a closed system for velocity only. The time derivative of density is found from the continuity equation (3.1*a*). In what follows we will consider the case when gravitational acceleration is directed along the negative y-axis, $\boldsymbol{g}=(0,-g)$ with $g>0$ as per figure 1(*a*).

Eliminating ρ' from (3.1), we get a vector wave-like equation for the velocity field:

$$\frac{\partial^2\boldsymbol{v}}{\partial t^2}=\frac{c_0^2}{\rho_0}[(\boldsymbol{\nabla}\rho_0+\rho_0\boldsymbol{\nabla})\boldsymbol{\nabla}\cdot\boldsymbol{v}+\boldsymbol{\nabla}(\boldsymbol{\nabla}\rho_0\cdot\boldsymbol{v})]-\widetilde{\boldsymbol{g}}\left[\boldsymbol{\nabla}\cdot\boldsymbol{v}+\frac{1}{\rho_0}\boldsymbol{\nabla}\rho_0\cdot\boldsymbol{v}\right], \tag{3.4}$$

where $\widetilde{\boldsymbol{g}}=\boldsymbol{g}-(\mathrm{d}^2p_0/\mathrm{d}\rho_0^2)\boldsymbol{\nabla}\rho_0$, and the term $\boldsymbol{\nabla}(\boldsymbol{\nabla}\rho_0\cdot\boldsymbol{v})$ clearly contains vorticity $\boldsymbol{\omega}=\boldsymbol{\nabla}\times\boldsymbol{v}$, which means that in the presence of stratification the flow is in general no longer irrotational. Equation (3.4) illustrates how gravity enters under two guises: (i) pure gravity effect in the term $\boldsymbol{g}\boldsymbol{\nabla}\cdot\boldsymbol{v}$, and (ii) through explicit density stratification, i.e. the terms involving $\boldsymbol{\nabla}\rho_0$. Depending on the physical situation, one of these two effects is dominant. Since we are interested in the interaction of sound waves with the horizontal interface rather than propagation through media, which has been studied before (Tolstoy 1963, 1965), for transparency we will first elaborate on the case (i) when the explicit base state density stratification can be neglected, $\boldsymbol{\nabla}\rho_0\simeq 0$, and also assume $\rho_0(\mathrm{d}^2p_0/\mathrm{d}\rho_0^2)/(\mathrm{d}p_0/\mathrm{d}\rho_0)\ll 1$, which allows us to neglect the variation of the sound speed c_0 with altitude y, for example, in the case of an ideal gas under

https://doi.org/10.1017/jfm.2018.897 Published online by Cambridge University Press

isothermal conditions. The condition $\boldsymbol{\nabla}\rho_0 \simeq 0$ is equivalent to assuming that ω_g is disparate from (either much smaller or much larger than) ω_g'. Then (3.4) for velocity $\boldsymbol{v}$ and the corresponding equation for density variation ρ' reduce to

$$\frac{\partial^2 \boldsymbol{v}}{\partial t^2} = c_0^2 \boldsymbol{\nabla}(\boldsymbol{\nabla}\cdot\boldsymbol{v}) - \boldsymbol{g}\boldsymbol{\nabla}\cdot\boldsymbol{v}, \quad \frac{\partial^2 \rho'}{\partial t^2} = c_0^2 \nabla^2 \rho' - \boldsymbol{g}\cdot\boldsymbol{\nabla}\rho'. \tag{3.5a,b}$$

Plugging the solution of the form $(uv)^{\mathrm{T}} = (\widehat{u}\,\widehat{v})^{\mathrm{T}} \mathrm{e}^{\mathrm{i}\psi}$ in (3.5*a*) leads to the dispersion relation

$$\omega^4 - [(\boldsymbol{k}\cdot\boldsymbol{k})c_0^2 - \mathrm{i}gk_y]\omega^2 = 0, \tag{3.6}$$

where we have used the notation $\boldsymbol{k}\cdot\boldsymbol{k}$ to differentiate from $|\boldsymbol{k}|^2$ as the wavenumber vector $\boldsymbol{k}$ is now complex as opposed to the classical case (§ 1). The dispersion relation (3.6) is the deep water limit of that for acoustic gravity waves with a free surface (Dalrymple & Rogers 2007; Kadri & Stiassnie 2013). Equation (3.6) yields two solutions: the travelling $\omega_1^2 = (\boldsymbol{k}\cdot\boldsymbol{k})c_0^2 - \mathrm{i}gk_y$ and standing $\omega_2^2 = 0$ waves, which apply in every medium with an appropriate speed of sound. The corresponding eigenvectors provide a relation between the velocity components:

$$\omega_1\colon \quad \widehat{v} = \widehat{u}(k_y - \mathrm{i}g/c_0^2)/k_x, \quad \omega_2\colon \quad \widehat{v} = -\widehat{u}k_x/k_y, \tag{3.7a,b}$$

i.e. the former is akin to the usual potential flow solution and the latter is a vorticity mode with the velocity vector $\boldsymbol{v}$ no longer parallel to that of the wavenumber $\boldsymbol{k}$.

Given that these modes are decoupled and we are interested in sound waves of non-vanishing frequency, we will focus on the 'potential flow' case (though a velocity potential as such does not exist). The dispersion relation (3.6) requires further interpretation since the wavenumber $\boldsymbol{k}$ is always complex as opposed to the classical case (§ 1). As follows from (3.6), if the y-component of the wavenumber is zero, then we arrive at the classical acoustic dispersion (1.3), i.e. $k_x c_0 = \omega$. This means that the gravity vector introduces an anisotropy: when $\boldsymbol{k} = (k_x, 0)$, gravity does not have any effect on the sound wave (in the same way as gravity does not change the horizontal velocity of a thrown stone), while for $\boldsymbol{k} = (0,\ k_y)$ the wavenumber becomes complex, with the imaginary part being responsible for decay/growth of the sound wave amplitude. In general, the direction of a plane sound wave, even in the presence of decay in a certain direction, is determined by the real part of the wavenumber vector, so that in our case $k_x \equiv k_x^{\mathrm{r}} = k\sin\theta$ and $k_y^{\mathrm{r}} = k\cos\theta$ are real, while $k_y = k_y^{\mathrm{r}} + \mathrm{i}k_y^{\mathrm{i}}$. Since $\boldsymbol{k}\cdot\boldsymbol{k} = k_x^2 + k_y^2$, then (3.6) yields

$$k_x = k\sin\theta, \quad k_y = \frac{\mathrm{i}g \pm \sqrt{-g^2 + 4c_0^2(\omega^2 - k_x^2 c_0^2)}}{2c_0^2}, \quad \text{where } k^2 = \frac{\omega^2}{c_0^2} - \frac{g^2}{4c_0^4}. \tag{3.8a,b}$$

Note that $k^2 \neq |\boldsymbol{k}|^2$. An important conclusion from the above formula for k_y and (3.7*a*) is that the x-component of the velocity experiences a jump across the interface since k_x is the same for all waves in both media, but the vertical velocity component is continuous based on (3.3*a*). Given the continuity of the x-component of the wavenumber, we derive a modified Snell's law:

$$\frac{k_x^i}{k_x^p} = 1 = \frac{k_i}{k_p}\frac{\sin\theta_1}{\sin\theta_2} = \frac{\sqrt{\omega^2/c_1^2 - g^2/4c_1^4}}{\sqrt{\omega^2/c_2^2 - g^2/4c_2^4}}\frac{\sin\theta_1}{\sin\theta_2} \quad \Rightarrow \quad \frac{\sin\theta_1}{\sin\theta_2} = \frac{c_1}{c_2}\frac{\sqrt{\omega^2 - g^2/4c_2^2}}{\sqrt{\omega^2 - g^2/4c_1^2}}, \tag{3.9}$$

https://doi.org/10.1017/jfm.2018.897 Published online by Cambridge University Press

which recovers the classical one (1.6) in the limit $g \to 0$. The case of pure gravity effect without surface tension leads to a concise expression for the Rayleigh reflection coefficient:

$$\frac{\widehat{u}_r}{\widehat{u}_i} = \frac{(g^2 + 4c_2^4k_2^2)(\mathrm{i}g - 2c_1^2k_1\cos\theta_1)\rho_2 - (g^2 + 4c_1^4k_1^2)(\mathrm{i}g - 2c_2^2k_2\cos\theta_2)\rho_1}{(g^2 + 4c_1^4k_1^2)(\mathrm{i}g - 2c_2^2k_2\cos\theta_2)\rho_1 - (g^2 + 4c_2^4k_2^2)(\mathrm{i}g + 2c_1^2k_1\cos\theta_1)\rho_2}, \tag{3.10}$$

where $k_{1,2}$ are given by (3.8) for the corresponding medium, and the angle θ_2 is found from (3.9).

Let us consider energy balance in the case treated here, i.e. when the explicit gradient of the base state density can be neglected in (3.1). Taking the scalar product of the velocity vector $\boldsymbol{v}$ with the momentum equation (3.1*b*) and using (3.2), we find

$$\frac{\partial}{\partial t}\left[\frac{1}{2}\rho_0\boldsymbol{v}\cdot\boldsymbol{v} + \frac{1}{2}\frac{p'^2}{\rho_0 c_0^2}\right] = -\boldsymbol{\nabla}\cdot(p'\boldsymbol{v}) + \boldsymbol{v}\cdot\boldsymbol{g}\frac{p'}{c_0^2}, \tag{3.11}$$

which shows the dynamic energy balance for a sound wave in some control volume D. The expression on the left is the sum of kinetic and potential compression energies, while the first term on the right is the energy flux $\boldsymbol{q} = p'\boldsymbol{v}$ through the boundary ∂D and the second term is the production of energy inside the volume D by the gravity force. Hence, the energy density flux is the same as in the classical case, though the expression for p' is different with the amplitude $\widehat{p} = \widehat{u}\omega\rho_0/k_x$. The behaviour of the reflection $\langle\mathcal{R}\rangle$ and transmission $\langle\mathcal{T}\rangle$ coefficients corresponding to (3.10) for averaged energy fluxes calculated with (2.2) is illustrated in figure 2(*b*) showing a significant shift in total reflection compared to the classical case if $\omega \sim \omega_g$ in accordance with (3.9), the physics of which is explained below. As we can also see from figure 2(*b*), the reflection coefficient increases and thus the transmission coefficient decreases due to the pure gravity effect, which should be contrasted to the recent observation (Godin 2006; Godin & Fuks 2012) of increased sound transmission from a point source if it is located close to the interface within a fraction of the wavelength and the base state density variation is taken into account. A possibility of an analogous behaviour in the context of the present analysis will be pointed out below when the case of density stratification is addressed.

To proceed with the energy considerations, note that the wave equation for the density variation (3.5*b*) is clearly not self-adjoint, thus having implications for energy balance. With the change of variable $\rho' = \mathrm{e}^{-\widehat{\boldsymbol{g}}\cdot\boldsymbol{x}/2}\widetilde{\rho}'$, where $\widehat{\boldsymbol{g}} = -\boldsymbol{g}/c_0^2$, (3.5*b*) reduces to a self-adjoint Klein–Gordon equation for particles with a non-zero mass (Fermi 1951): $\partial^2\widetilde{\rho}'/\partial t^2 = c_0^2\nabla^2\widetilde{\rho}' - \widetilde{\rho}'|\boldsymbol{g}|^2/4c_0^2$, as opposed to the massless D'Alembert equation (1.1). Letting $\widetilde{\rho}' \sim \mathrm{e}^{\mathrm{i}(\boldsymbol{k}\cdot\boldsymbol{x}-\omega t)}$, we recover the gravity-modified dispersion relation (3.8). Also, following the analysis of § 1, with $\widetilde{\rho}' = \widehat{\rho}'(y)\mathrm{e}^{\mathrm{i}(k_x x-\omega t)}$ we get another stationary 1D Schrödinger equation $\widehat{\rho}'_{yy} + (\omega^2/c^2 - k_x^2 - g^2/4c_0^4)\widehat{\rho}' = 0$, from which it follows that the potential barrier size

$$V \sim [\omega^2/c^2 - g^2/4c^4]_2^1 \tag{3.12}$$

differs from the classical case (§ 1), affecting not only the total reflection angle θ_c, but also the reflection/transmission even when the phonon energy $E > V$. Owing to the conservative nature of gravity, the total energy balance is still the same, $\langle\mathcal{R}\rangle + \langle\mathcal{T}\rangle = 1$. The mass-like effect of gravity explains the increased reflection in figure 2(*b*) for the configuration shown in figure 1(*a*).

https://doi.org/10.1017/jfm.2018.897 Published online by Cambridge University Press

It is important to remark that, in the presence of stratification, $\nabla\rho_0 \neq 0$, but when the sound speed variation is neglected, (3.4) admits the potential flow ($\boldsymbol{v} = \nabla\phi$) formulation (Bondi 1947; Abdolali & Kirby 2017)

$$\frac{\partial^2\phi}{\partial t^2} = c_0^2\nabla^2\phi + g\frac{\partial\phi}{\partial y}, \tag{3.13}$$

which leads to exactly the same travelling wave solution as the dispersion relation (3.6) in the above considered case (i) of the pure gravity effect and hence the same modified Snell's law (3.9).

In the general case, however, when both density stratification and sound speed variation are taken into account (3.4), the initially plane wave neither stays plane nor preserves its direction due to refraction (Brekhovskikh 1960), which can be easily seen if one approximates the continuous stratification by discrete layers with different sound speeds and then applies (3.9). Hence, in this case the universality of a Snell's type law is lost – the angle of incidence at a particular point of the interface depends not only on the initial direction of the plane wave, but also on the distance travelled and the particularities of the sound speed variation. Nevertheless, the dispersion relation corresponding to (3.4) provides leading-order corrections (expanded here for small $\dot\rho_0$, $\ddot\rho_0$ and g assuming slow variation of ρ_0 with y, so that $\omega_{1,2}$ and k_y are slow functions of y as well) to the frequencies $\omega_{1,2}$ determined above:

$$\omega_1^2 = (\boldsymbol{k}\cdot\boldsymbol{k})c_0^2 - \mathrm{i}\widetilde{g}k_y - 2\mathrm{i}k_y c_0^2\frac{\dot\rho_0}{\rho_0} - \frac{c_0^2k_y^2}{(\boldsymbol{k}\cdot\boldsymbol{k})}\frac{\ddot\rho_0}{\rho_0}, \quad \omega_2^2 = -\frac{c_0^2k_x^2}{(\boldsymbol{k}\cdot\boldsymbol{k})}\frac{\ddot\rho_0}{\rho_0}, \tag{3.14a,b}$$

where k_y is general, not undisturbed wavenumber component, and $\widetilde{g} = g - (\mathrm{d}^2p_0/\mathrm{d}\rho_0^2)\dot\rho_0$. Thus, the standing wave solution for $\nabla\rho_0 \simeq 0$ is no longer standing for $\nabla\rho_0 \neq 0$, with the corresponding eigenvectors again accounting for the potential and vorticity modes:

$$\omega_1\text{:}\quad \widehat{v} = \widehat{u}\frac{k_y}{k_x}\left(1 - \frac{\gamma}{k_y} - \mathrm{i}\frac{\widetilde{g}}{c_0^2k_y}\right), \tag{3.15a}$$

$$\omega_2\text{:}\quad \widehat{v} = -\widehat{u}\frac{k_x}{k_y}\left(1 + \frac{\gamma}{k_y}\right), \quad \text{where } \gamma = \mathrm{i}\frac{\dot\rho_0}{\rho_0} + \frac{k_y}{(\boldsymbol{k}\cdot\boldsymbol{k})}\frac{\ddot\rho_0}{\rho_0}. \tag{3.15b}$$

Since the x-component of the wavenumber $\boldsymbol{k}$ is real and given upon arrival at the interface, from (3.14a) we can find the y-component of the corresponding wavenumber expanded here for both small base state density variations and gravity:

$$k_y = k_{0y}\left(\pm1 - \frac{c_0^2}{2\omega^2}\frac{\ddot\rho_0}{\rho_0}\right) + \mathrm{i}\frac{\dot\rho_0}{\rho_0} + \mathrm{i}\frac{g}{2c_0^2} + O(g^2), \quad k_{0y} = \sqrt{(\omega/c_0)^2 - k_x^2}, \tag{3.16}$$

where k_{0y} is the undisturbed y-component of the wavenumber in the absence of gravity (1.5). Given the relation between $\widehat{u}$ and $\widehat{v}$, we can solve (3.3) perturbatively for the amplitudes of the reflected and refracted waves in the presence of surface tension, e.g. the correction $\delta\widehat{u}_r$ to $\widehat{u}_r$ given by (2.1), so that the total solution is $\widehat{u}_r + \delta\widehat{u}_r$, with the singled out effect of density stratification reads

$$\frac{\delta\widehat{u}_r}{\widehat{u}_i} = -k_y\kappa_y\omega^2\frac{(\boldsymbol{\kappa}\cdot\boldsymbol{\kappa})(\mathrm{i}k_x\kappa_y\sigma + \omega^2\rho_2)\ddot\rho_1 - (\boldsymbol{k}\cdot\boldsymbol{k})\omega^2\rho_1\ddot\rho_2}{(\boldsymbol{k}\cdot\boldsymbol{k})(\boldsymbol{\kappa}\cdot\boldsymbol{\kappa})[\kappa_y(\mathrm{i}k_x^2k_y\sigma + \omega^2\rho_1) + k_y\omega^2\rho_2]^2}, \tag{3.17}$$

https://doi.org/10.1017/jfm.2018.897 Published online by Cambridge University Press

which is real-valued for $\sigma = 0$, and with the pure gravity effect (no explicit stratification) reads

$$\frac{\delta\widehat{u}_r}{\widehat{u}_i} = k_y\rho_1 \frac{\sigma[k_x^4\kappa_y - (\boldsymbol{k}\cdot\boldsymbol{k})k_x^2\kappa_y + k_x^2k_y\kappa_y^2] - \mathrm{i}\omega^2[(\boldsymbol{\kappa}\cdot\boldsymbol{\kappa})\rho_1 - (\boldsymbol{k}\cdot\boldsymbol{k})\rho_2]}{[\kappa_y(\mathrm{i}k_x^2k_y\sigma + \omega^2\rho_1) + k_y\omega^2\rho_2]^2} g, \tag{3.18}$$

which for $\sigma = 0$ is imaginary and tends to zero with increasing frequency ω as opposed to (3.17). Both corrections may vanish depending on the incident k_y and transmitted κ_y wavenumbers as well as the density distribution of both media. The buoyancy effects $\dot{\rho}_{1,2}$ proved to be irrelevant in the leading-order correction to the reflection coefficient. As follows from (3.17), transmission may increase (and thus reflection decrease) depending on stratifications in both media similar to the observation by Godin (2006) and Godin & Fuks (2012), though the problem formulation in the latter works differs from the present one as pointed out earlier. While the coefficients $\langle\mathcal{R}\rangle$ and $\langle\mathcal{T}\rangle$ corresponding to (3.17) are easy to compute, their interpretation can be done only in the context of a concrete choice of stratification, which is beyond the scope of the present study.

4. Viscosity effects

The decoupled acoustic equations with inclusion of viscous effects (in the absence of gravity) are

$$\frac{\partial^2\rho'}{\partial t^2} = \left[c_0^2 + \frac{1}{\rho_0}\left(\lambda + \frac{4}{3}\mu\right)\frac{\partial}{\partial t}\right]\Delta\rho', \tag{4.1a}$$

$$\frac{\partial^2\boldsymbol{v}}{\partial t^2} = \left[c_0^2 + \frac{1}{\rho_0}\left(\lambda + \frac{4}{3}\mu\right)\frac{\partial}{\partial t}\right]\Delta\boldsymbol{v} + \left[c_0^2 + \frac{\mu}{\rho_0}\frac{\partial}{\partial t}\right]\boldsymbol{\nabla}\times\boldsymbol{\omega}, \tag{4.1b}$$

where μ and λ are shear and bulk viscosities, respectively. Plugging in (4.1*b*) the anzatz $(uv)^{\mathrm{T}} = (\widehat{u}\,\widehat{v})^{\mathrm{T}}\mathrm{e}^{\mathrm{i}(\boldsymbol{k}\cdot\boldsymbol{x}-\omega t)}$ furnishes the dispersion relation

$$\left\{\omega^2 - (\boldsymbol{k}\cdot\boldsymbol{k})\left[c_0^2 - \frac{\mathrm{i}\omega}{\rho_0}\left(\lambda + \frac{4}{3}\mu\right)\right]\right\}\left\{\omega^2 + (\boldsymbol{k}\cdot\boldsymbol{k})\frac{\mathrm{i}\omega}{\rho_0}\left(\lambda + \frac{1}{3}\mu\right)\right\} = 0. \tag{4.2}$$

In the case of a freely propagating sound wave, isotropy of the viscosity action naturally follows, i.e. we must assume that both $k_x = k_x^{\mathrm{r}} + \mathrm{i}k_x^{\mathrm{i}}$ and $k_y = k_y^{\mathrm{r}} + \mathrm{i}k_y^{\mathrm{i}}$ have real and imaginary components. The direction of the plane wave is determined by the real parts $k_x^{\mathrm{r}} = k_{\mathrm{r}}\sin\theta$ and $k_y^{\mathrm{r}} = k_{\mathrm{r}}\cos\theta$ and isotropy dictates that analogous expressions hold for the imaginary parts $k_x^{\mathrm{i}} = k_{\mathrm{i}}\sin\theta$ and $k_y^{\mathrm{i}} = k_{\mathrm{i}}\cos\theta$ responsible for the (homogeneous) decay of the sound wave due to viscosity. Therefore, the analysis of the dispersion relation reduces to a single dimension since $\boldsymbol{k}\cdot\boldsymbol{k} = k_x^2 + k_y^2 = k_{\mathrm{r}}^2 - k_{\mathrm{i}}^2 + 2\mathrm{i}k_{\mathrm{r}}k_{\mathrm{i}}$, i.e. only for one complex wavenumber $k = k_{\mathrm{r}} + \mathrm{i}k_{\mathrm{i}}$. Linearizing for small values of viscosities, we get a system of two equations for k_{r} and k_{i}:

$$\omega^2/c_0^2 = k_{\mathrm{r}}^2 - k_{\mathrm{i}}^2, \quad 2k_{\mathrm{r}}k_{\mathrm{i}} = (\lambda + 4/3\mu)\omega^3/\rho_0c_0^4 \equiv b. \tag{4.3a,b}$$

From the latter equation it follows that either $k_{\mathrm{r}} > 0$ and $k_{\mathrm{i}} > 0$ or $k_{\mathrm{r}} < 0$ and $k_{\mathrm{i}} < 0$, i.e. the direction of the wave propagation correlates with the direction of decay. Solving (4.3) we find $k_{\mathrm{r}}^2 = (\omega^2/2c_0^2)[1 \pm \sqrt{1 + b^2c_0^4/\omega^4}]$, $k_{\mathrm{i}}^2 = k_{\mathrm{r}}^2 - \omega^2/c_0^2$, where we chose the plus sign since k_{r} must be real; the corresponding x- and y-components of

https://doi.org/10.1017/jfm.2018.897 Published online by Cambridge University Press

the real and imaginary parts of the two-dimensional wavenumber are then determined by multiplying k with $\sin\theta$ and $\cos\theta$, respectively. Obviously, in such a general setting the standard analysis (§ 1) does not apply due to the decay of the signal in the x-direction: amplitudes now depend on x and hence the problem should be treated back in physical space. The only two situations (cf. figure 1*c*) when the standard analysis would be relevant are: (i) the plane wave emitted with varying amplitude along the phase $\psi = \boldsymbol{k}^{\mathrm{r}} \cdot \boldsymbol{x} - \omega t = \text{const.}$ (the closer to the interface, the lower the amplitude at the source location), so that the amplitude of the sound wave arriving at the interface is the same at all x locations effectively meaning that $k_x^{\mathrm{i}} = 0$; and (ii) a sufficiently narrow sound beam (a ray), so that the decay is negligible in the neighbourhood of its intersection with the interface (for angles of incidence away from grazing) as long as $d \ll c_0\lambda^2/\nu$, where λ is the sound wavelength and d the beam diameter. Together with the condition of negligible divergence of the beam based on Huygens' principle, we can quantify setting (ii):

$$\sqrt{l\lambda} \ll d \ll c_0\lambda^2/\nu, \tag{4.4}$$

where l is the beam length. Since $k_x^{\mathrm{i}} = 0$ and k_y^{i} is small for low-viscosity fluids, we get

$$k^2 = \omega^2/c_0^2, \quad k_y^{\mathrm{i}} = b/(2k\cos\theta), \tag{4.5a,b}$$

where in the latter expression one must assume $b \ll k\cos\theta$, which becomes impossible for $\theta \to \pi/2$ since the magnitude of k is fixed. It is easy to show that this restriction is not related to linearization for small viscosity, but, in fact, is a property of the original system: as $\theta \to \pi/2$ it becomes impossible to deliver the same amplitude (not decaying in x) signal to the interface over longer distance through the viscous dissipating fluid. The first bracket in (4.2) gives the standard potential flow result for ω_1 with the corresponding y-component of the wavenumber:

$$\omega_1\colon \quad \widehat{v} = \widehat{u}\frac{k_y}{k_x}, \quad k_y = \pm k_{0y}\left(1 + \frac{\mathrm{i}}{2}\frac{\omega^3\left(\lambda + \frac{4}{3}\mu\right)}{\rho_0 c_0^4 k_{0y}^2} + \cdots\right), \tag{4.6}$$

where the expression for k_y is valid provided the condition

$$\frac{\omega^3}{\rho_0 c_0^4}\left(\lambda + \frac{4}{3}\mu\right) \ll k_{0y}^2 \quad \Rightarrow \quad \lambda_{0y}^2 \equiv \left(\frac{2\pi}{k_{0y}}\right)^2 \ll \frac{4\pi^2\rho_0 c_0^4}{\omega^3}\left(\lambda + \frac{4}{3}\mu\right)^{-1} \tag{4.7}$$

is satisfied. The second bracket in (4.2) gives the vorticity-type solution ω_2 denoted by the wavenumbers $\boldsymbol{k}_r'$ and $\boldsymbol{k}_p'$ in figure 1(*a*) with the corresponding y-component:

$$\omega_2\colon \quad \widehat{v} = -\widehat{u}\frac{k_x}{k_y}, \quad k_y = \pm \mathrm{e}^{\mathrm{i}(\pi/4)}\left(\frac{\rho_0\omega}{\lambda + \frac{1}{3}\mu}\right)^{1/2}\left[1 + \mathrm{i}\frac{k_x^2}{2}\frac{\lambda + \frac{1}{3}\mu}{\rho_0\omega} + \cdots\right], \tag{4.8}$$

which is a fast decaying (in space) mode for low-viscosity fluids, where we take the plus sign for medium 2 (transmitted mode) and minus sign for medium 1 (reflected mode). This last mode is instrumental in resolving the problem of acoustic reflection/refraction – without it, i.e. assuming that the acoustic field is potential $\boldsymbol{v} = \nabla\phi$, we get an overdetermined system, which physically means that interaction of an oblique acoustic field with the fluid interface generates vorticity in analogy to

https://doi.org/10.1017/jfm.2018.897 Published online by Cambridge University Press

an acoustic boundary layer in the reflection from a solid wall as alluded to by Pierce (1989). However, this mode vanishes for normal incidence, $\theta_1 \to 0$, as then $\boldsymbol{\omega} = 0$.

The corresponding linearized interfacial conditions, with $\boldsymbol{\tau}$ being the viscous stress tensor, read

$$y = 0: \qquad [v]_1^2 = 0, \quad h_t = v, \tag{4.9a}$$

$$[p' - \boldsymbol{n}\cdot\boldsymbol{\tau}\cdot\boldsymbol{n}]_1^2 = \sigma h_{xx}, \quad \text{where } \boldsymbol{n}\cdot\boldsymbol{\tau}\cdot\boldsymbol{n} = (\lambda - 2\mu/3)(u_x + v_y) + 2\mu v_y, \tag{4.9b}$$

$$[\boldsymbol{t}\cdot\boldsymbol{\tau}\cdot\boldsymbol{n}]_1^2 = 0, \quad \text{where } \boldsymbol{t}\cdot\boldsymbol{\tau}\cdot\boldsymbol{n} = \mu(u_y + v_x), \tag{4.9c}$$

$$[u]_1^2 = 0, \tag{4.9d}$$

i.e. in (3.3) we have replaced (3.3*b*) by the normal stress balance (4.9*b*), and added the tangential stress balance (4.9*c*) along with the no-slip condition (4.9*d*). Pressure p' in (4.9*b*) is found from (3.2) and the linearized continuity equation (3.1*a*), where $\rho_0 = \text{const}$. With the ansatz $(uv)^{\mathrm{T}} = (\widehat{u}\,\widehat{v})^{\mathrm{T}}\mathrm{e}^{\mathrm{i}(\boldsymbol{k}\cdot\boldsymbol{x}-\omega t)}$ we first arrive at

$$\frac{\partial \rho'}{\partial t} = -\rho_0 \nabla\cdot\boldsymbol{v} = -\mathrm{i}\rho_0(k_x\widehat{u} + k_y\widehat{v})\mathrm{e}^{\mathrm{i}(\boldsymbol{k}\cdot\boldsymbol{x}-\omega t)} \quad \Rightarrow \quad \rho' = -\mathrm{i}\frac{\rho_0}{\omega}\nabla\cdot\boldsymbol{v}, \tag{4.10}$$

so that $\widehat{\rho} = (k_x\widehat{u} + k_y\widehat{v})\rho_0/\omega$ and then $p' = c_0^2\rho'$ with $\widehat{p} = (k_x\widehat{u} + k_y\widehat{v})\rho_0 c_0^2/\omega$ as per the adiabatic assumption (3.2). Altogether, we have five equations – two kinematic (4.9*a*), dynamic normal (4.9*b*), dynamic tangent (4.9*c*) and no-slip (4.9*d*) boundary conditions – for the interfacial amplitude $\widehat{h}$, two reflected waves $(\widehat{u}_r, \widehat{v}_r)$ and $(\widehat{u}'_r, \widehat{v}'_r)$, and two refracted waves $(\widehat{u}_p, \widehat{v}_p)$ and $(\widehat{u}'_p, \widehat{v}'_p)$. Note that the components in each pair $(\widehat{u}_m, \widehat{v}_m)$ are related via either (4.6) or (4.8) depending on the nature of the acoustic wave. Finally, the energy density flux in the classical acoustic case $\boldsymbol{q} = p'\boldsymbol{v}$ is modified to $\boldsymbol{q} = p'\boldsymbol{v} - \boldsymbol{v}\cdot\boldsymbol{\tau}$ (Landau & Lifshitz 1987). Using the condition of velocity continuity across the interface (no slip), which dictates the continuity of the real part of k_x, leads to the modification of Snell's law (1.6) stated here along with the corresponding potential barrier V as per the stationary 1D Schrodinger analysis (§ 1) applied to (4.1*a*) with $\rho' = \widetilde{\rho}'(y)\mathrm{e}^{\mathrm{i}(k_x x-\omega t)}$ yielding $\widetilde{\rho}'_{yy} + [\omega^2\beta/c_0^2 - k_x^2]\widetilde{\rho}' = 0$:

$$\frac{\sin\theta_1}{\sin\theta_2} = \frac{c_1}{c_2}\frac{1 + \dfrac{\omega^2}{8\rho_2^2 c_2^4}\left(\lambda_2 + \dfrac{4}{3}\mu_2\right)^2}{1 + \dfrac{\omega^2}{8\rho_1^2 c_1^4}\left(\lambda_1 + \dfrac{4}{3}\mu_1\right)^2}; \qquad V \sim \left[\frac{\omega^2\beta}{c^2}\right]_2^1, \qquad \beta = \frac{c^2 + \dfrac{\mathrm{i}\omega}{\rho}\left(\lambda + \dfrac{4}{3}\mu\right)}{c^2 + \dfrac{\omega^2}{\rho^2 c^2}\left(\lambda + \dfrac{4}{3}\mu\right)^2}, \tag{4.11a,b}$$

both exhibiting significant departures from the classical case (§ 1); notably, V is complex now with the imaginary part being responsible for adsorption.

First, let us consider the case when both viscosities are small and of the same order, $\mu_1 = O(\mu_2)$. In the case of one medium only (so that ρ_2 and μ_2 both vanish), the potential flow correction (4.6) of (2.1) due to viscosity reads

$$\frac{\delta\widehat{u}_r}{\widehat{u}_i} = -\sigma\omega\left(\mu_1 + \frac{4}{3}\lambda_1\right)\frac{k_x^2(k_x^2 - k_y^2)^2}{k_y(\mathrm{i}\sigma k_y k_x^2 + \omega^2\rho_1)^2}, \tag{4.12}$$

where here and in the following expressions k_y and κ_y are undisturbed wavenumbers. The interesting fact is that (4.12) vanishes in the absence of surface tension, that is, reflection is the same as if medium 1 is inviscid. However, retaining inertia of

https://doi.org/10.1017/jfm.2018.897 Published online by Cambridge University Press

medium 2, as follows from the discussion below, leads to a non-zero correction. In the case of increasing incidence angle θ_1, k_y decreases and thus the correction (4.12) grows, which is the consequence of increasing effect of viscosity due to enhanced friction/shear with the interface (especially when a sound wave propagates close to parallel to it), but k_y is bound from below as per the restriction (4.7). When both media are present, without bulk viscosity, in the near-normal incidence case, $\theta_1 \to 0$ and thus $k_x \to 0$, we find

$$\frac{\delta\widehat{u}_r}{\widehat{u}_i} = \frac{4\mathrm{i}k_y\kappa_y}{3\omega}\frac{\mu_1\rho_2k_y^2 - \mu_2\rho_1\kappa_y^2}{(\kappa_y\rho_1 + k_y\rho_2)^2} + O(k_x^2), \tag{4.13}$$

i.e. the leading-order term does not depend on surface tension. The limit of $\mu_2 \to 0$ does not lead to vanishing $\delta\widehat{u}_r$ if one retains the inertia of the second medium, $\rho_2 \neq 0$. In the near-normal incidence case the correction to the reflection coefficient $\langle\mathcal{R}\rangle - \langle\mathcal{R}_0\rangle$ corresponding to (4.13) then becomes

$$-\frac{16\omega^2(\rho_1c_1^2\mu_2 - \rho_2c_2^2\mu_1)[2\rho_1^3c_1^4\mu_2 - 2\rho_2^3c_2^4\mu_1 + 3\rho_1\rho_2c_1^2c_2^2(\rho_1\mu_1 - \rho_2\mu_2)]}{9\rho_1\rho_2c_1^3c_2^3(\rho_1c_1 + \rho_2c_2)^4}, \tag{4.14}$$

which changes sign at $\mu_1/\mu_2 = (2\rho_1^2c_1^2 - 3\rho_2^2c_2^2)/(2\rho_2^2c_2^2 - 3\rho_1^2c_1^2)$ and at $\mu_1/\mu_2 = \rho_1c_1^2/\rho_2c_2^2$. Figures 2(*c*) and 2(*d*) demonstrate both positive and negative cases of (4.14) confirming the trend suggested by (4.13) that viscosity may both enhance and suppress reflection/transmission due to the imaginary part of the potential barrier (4.11*b*), which effectively makes it active. Therefore, even though an infinitesimally thin (Gibbs) interface cannot accumulate energy, the energy density flux of the reflected and transmitted modes is not conserved $\langle\mathcal{R}\rangle + \langle\mathcal{T}\rangle < 1$, cf. figure 2(*c*,*d*). These same plots indicate that transmission increases with the incidence angle θ_1 – this behaviour is analogous to increasing adsorption with θ_1 in the reflection of a plane acoustic wave from a solid wall (Pierce 1989). Without both surface tension and bulk viscosities and when there is viscous stratification, $\mu_2 \ll \mu_1$, the correction to (1.4*a*) is of the form

$$\begin{aligned}\frac{\delta\widehat{u}_r}{\widehat{u}_i} = {} & \frac{(1+\mathrm{i})\rho_2}{3\omega k_y(k_y\rho_2 + \kappa_y\rho_1)^2}\Big\{2(1+\mathrm{i})\kappa_y\mu_1(k_x^2 - k_y^2)^2 \\ & + \mathrm{i}\sqrt{6}\omega^{1/2}k_x^2k_y^2\sqrt{\rho_2\mu_2}(\sqrt{\rho_1/\rho_2} - \sqrt{\rho_2/\rho_1})^2\Big\} + O[(\mu_2/\mu_1)^{3/2}].\end{aligned} \tag{4.15}$$

The secondary reflected mode (4.8) amplitude, which is of rotational type, in the absence of surface tension and bulk viscosities and for $\mu_1 = O(\mu_2)$, reads

$$\frac{\widehat{u}'_r}{\widehat{u}_i} = 2k_y\frac{\rho_1 - \rho_2}{(\kappa_y\rho_1 + k_y\rho_2)(1 + \sqrt{\rho_1\mu_1/\rho_2\mu_2})} + O(\mu_1, \mu_2), \tag{4.16}$$

and vanishes when $\rho_1 - \rho_2 = 0$. As follows from (4.16), lowering μ_1/μ_2 increases the amplitude of this vorticity mode, which (due to energy conservation) reduces the reflection of an acoustic wave as seen in figure 2(*c*). In the case of viscous stratification, $\mu_2 \ll \mu_1$, we get

$$\frac{\widehat{u}'_r}{\widehat{u}_i} = 2k_y\frac{(\rho_1 - \rho_2)\sqrt{\rho_2\mu_2/\rho_1\mu_1} + \sqrt{2/3}(1-\mathrm{i})\kappa_y\sqrt{\rho_1\mu_1/\omega}}{\kappa_y\rho_1 + k_y\rho_2} + O(\mu_2/\mu_1), \tag{4.17}$$

https://doi.org/10.1017/jfm.2018.897 Published online by Cambridge University Press

which diverges at low frequencies $\omega \to 0$. The frequency at which the effect of the vorticity mode (4.17) is $O(1)$, i.e. $\widehat{u}_r' \sim \widehat{u}_i$, is found from $k\sqrt{\mu/\omega\rho} \sim 1$, which gives $\omega \sim c^2/\nu \equiv \omega_\nu$; e.g. for water the frequency $f = \omega/2\pi$ is far in the ultrasound range $\simeq 10^{11}$ Hz, for glycerol $\simeq 10^9$ Hz, and for air $\simeq 10^{10}$ Hz. For rarefied gases, we can estimate $\omega_\nu \sim c^2/\nu \sim \mathcal{S}\rho_N c \sim \mathcal{S}\rho_N\sqrt{k_B T}$, where ρ_N is molecular density and $\mathcal{S}$ the effective collision cross-section. Thus, the critical frequency ω_ν decreases when ρ_N is lowered, making the vorticity effect more pronounced and observable at common frequencies. Also, for rarefied gases, thermal conductivity is estimated as $\lambda_T \sim c_V \mu$ and hence thermal diffusivity $\alpha \sim \mu/\rho = \nu$, thus prompting us to revisit the adiabatic assumption (3.2). Because the equation of state is linear for waves of small amplitude, then both pressure and temperature vary as $\sim\sin(kx - \omega t)$. Given the sound wavelength λ, the regions of high and low pressure (and thus of temperature) are separated by a distance $\lambda/2$. Hence, the condition for validity of (3.2) is that negligible heat flow should occur between these two regions in the course of a half-period π/ω of the wave during which the temperature distribution is reversed. Since the distance over which heat diffuses in time t is $(\alpha t)^{1/2}$, the assumption (3.2) is valid provided (Fletcher 1974)

$$(\alpha\pi/\omega)^{1/2} \ll \lambda/2 \quad \Rightarrow \quad \omega \ll \pi c^2/\alpha \equiv \omega_a. \tag{4.18}$$

For air we find $f = \omega/2\pi \ll c^2/\alpha \simeq 10^{10}$ Hz. Hence, for (rarefied) gases, the frequency ω_a at which the adiabatic assumption fails is of the same order as the frequency ω_ν at which the vorticity mode becomes important. The condition under which the vorticity mode will appear while the assumption (3.2) remains valid, i.e. when $\omega_\nu \ll \omega_a$, is for the Prandtl number to be $Pr = \nu/\alpha \gg 1$. While for gases $Pr = 0.7$–1, for water $Pr = 1$–10 and for oils $Pr = 50$–2000, i.e. for the latter media no generalization of the sound propagation theory to the non-adiabatic case is needed as follows from (4.18).

5. Conclusions and further comments

Revisiting the classical Snell's law (1.6) with the goal to include the ubiquitous physical effects – viscosity, surface tension and gravity – generalized the classical analysis (Landau & Lifshitz 1987) and revealed not only modified laws of refraction (3.9) and (4.11*a*), which are now dispersive (frequency-dependent) and explained here with the help of the corresponding potential barriers (3.12) and (4.11*b*), but also other phenomena, in particular surface tension enhancing reflection, acoustic field generating vorticity near the interface between fluids, and viscosity enhancing/suppressing reflection as well as giving rise to extra reflected and transmitted waves. The latter observation is analogous to the Klein paradox (Klein 1929; Dombey & Calogeracos 1999), in which the potential barrier emits electron–positron pairs when an electron of mass m and energy E is incident on the potential barrier $V > E + m$. The complex nature of V in the presence of viscosity (4.11*b*) also explains energy losses, $\langle\mathcal{R}\rangle + \langle\mathcal{T}\rangle < 1$.

In summary, the effects of gravity, surface tension and viscosity can be considered separately provided the characteristic frequencies defined in § 1 are disparate:

$$\omega_g \ll \omega_\sigma \ll \omega_\nu, \tag{5.1}$$

and therefore lead to separation of the corresponding time scales. Each effect becomes relevant when the acoustic wave frequency ω is comparable to the corresponding characteristic frequency in either medium. Surface tension proved not to affect the

https://doi.org/10.1017/jfm.2018.897 Published online by Cambridge University Press

classical Snell's law, but the reflection and transmission coefficients do change. The pure gravity effect $\omega \sim \omega_g$, i.e. when the base state density stratification is neglected, can be considered in isolation provided ω_g is either much larger or much smaller than ω_g' and ω_g''. The corresponding Snell's law (3.9) remains valid, however, even when $\omega_g \sim \omega_g'$ as long as the speed of sound does not vary appreciably. Viscosity also modifies the Snell's law to (4.11*a*) with the adiabatic approximation for sound propagation (3.2) justified in the viscous case $\omega \sim \omega_\nu$ provided $Pr \gg 1$. In some particular situations, depending on the fluid properties the characteristic frequencies may becomes comparable, e.g. $\omega_\sigma \sim \omega_\nu$ requires $\mu \sim \sigma/c$, which is conceivable for some liquids.

While here we focused on the phenomena admitting universal refraction laws in order to make the comparison to the classical Snell's law (1.6) transparent, among the questions requiring further study are relaxing the conditions (3.2) and (4.7) in the viscous case and accounting for the effects of sound speed variation in continuously stratified fluids (Zhang & Swinney 2017), for example, in the case of water as dictated by Tait's equation of state. Relaxing the adiabatic assumption (3.2) in the viscous case should lead to the existence of entropy waves decaying fast similar to the vorticity waves near a solid boundary (Pierce 1989). Also, we naturally considered the systems homogeneous in the x-direction (along the interface), which enabled conservation of the corresponding component of the momentum and hence that of the wavenumber (Landau & Lifshitz 1987). However, in the geophysical context the x invariance is broken by the seabed topography such as a shelf break, which together with the finite depth of the ocean may lead to the generation of a countable infinity of reflected and transmitted modes (Kadri & Stiassnie 2012).

Acknowledgements

This work was partially supported by the Natural Sciences and Engineering Research Council of Canada (NSERC) under grant no. 6186. The author would also like to thank A. Zelnikov for stimulating discussions and G. M. Homsy for feedback on the manuscript.

REFERENCES

ABDOLALI, A. & KIRBY, J. T. 2017 Role of compressibility on tsunami propagation. *J. Geophys. Res. Oceans* **122**, 9780–9794.

ABDOLALI, A., KIRBY, J. T. & BELLOTTI, G. 2015 Depth-integrated equation for hydro-acoustic waves with bottom damping. *J. Fluid Mech.* **766**, R1.

BONDI, H. 1947 Waves on the surface of a compressible liquid. *Proc. Camb. Phil. Soc.* **43**, 75–95.

BREKHOVSKIKH, L. M. 1960 *Waves in Layered Media*. Academic Press.

DAHL, P. H. 2007 High-frequency underwater sound. In *Wiley Encyclopedia of Electrical and Electronics Engineering*, pp. 1–19. John Wiley.

DALRYMPLE, R. A. & ROGERS, B. D. 2007 A note on wave celerities on a compressible fluid. In *Proceedings of the 30th International Conference on Coastal Engineering (ICCE) 2006, San Diego, CA* (ed. J. M. Smith), pp. 3–13. World Scientific.

DOMBEY, N. & CALOGERACOS, A. 1999 Seventy years of the Klein paradox. *Phys. Rep.* **315**, 41–58.

DRINKWATER, B. W. 2016 Dynamic-field devices for the ultrasonic manipulation of microparticles. *Lab on a Chip* **16**, 2360–2375.

FERMI, E. 1951 *Elementary Particles*. Yale University Press.

FLETCHER, N. H. 1974 Adiabatic assumption for wave propagation. *Am. J. Phys.* **42**, 487–489.

GODIN, O. A. 2006 Anomalous transparency of water–air interface for low-frequency sound. *Phys. Rev. Lett.* **97**, 164301.

https://doi.org/10.1017/jfm.2018.897 Published online by Cambridge University Press

GODIN, O. A. & FUKS, I. M. 2012 Transmission of acoustic-gravity waves through gas–liquid interfaces. *J. Fluid Mech.* **709**, 313–340.

KADRI, U. & STIASSNIE, M. 2012 Acoustic-gravity waves interacting with the shelf break. *J. Geophys. Res.* **117**, C03035.

KADRI, U. & STIASSNIE, M. 2013 Generation of an acoustic-gravity wave by two gravity waves, and their subsequent mutual interaction. *J. Fluid Mech.* **735**, R6.

KINSLER, L. E., FREY, A. R., COPPENS, A. B. & SANDERS, J. V. 1999 *Fundamentals of Acoustics*. Wiley.

KLEIN, O. 1929 Die Reflexion von Elektronen an einem Potentialsprung nach der Relativistischen Dynamik von Dirac. *Z. Phys.* **53**, 157–165.

LANDAU, L. D. & LIFSHITZ, E. M. 1987 *Fluid Mechanics*. Pergamon Press.

MUNK, W. H., SPINDEL, R. C., BAGGEROER, A. & BIRDSALL, T. G. 1994 The Heard Island feasibility test. *J. Acoust. Soc. Am.* **96**, 2330–2342.

PAPADAKIS, E. P. 1999 *Ultrasonic Instruments and Devices*. Academic Press.

PIERCE, A. D. 1989 *Acoustics: An Introduction to its Physical Principles and Applications*. Acoustical Society of America.

TOLSTOY, I. 1963 The theory of waves in stratified fluids including the effects of gravity and rotation. *Rev. Mod. Phys.* **35**, 207–230.

TOLSTOY, I. 1965 Effect of density stratification on sound waves. *J. Geophys. Res.* **70**, 6009–6015.

WATSON, T. & YOUNG, S. R. 2008 Therapeutic ultrasound. In *Electrotherapy: Evidence-based Practice*, pp. 179–200. Churchill Livingstone.

WHITAKER, R. W. & NORRIS, D. E. 2008 Infrasound propagation. In *Handbook of Signal Processing in Acoustics*, pp. 1497–1519. Springer.

ZHANG, L. & SWINNEY, H. L. 2017 Sound propagation in a continuously stratified laboratory ocean model. *J. Acoust. Soc. Am.* **141**, 3186–3189.

https://doi.org/10.1017/jfm.2018.897 Published online by Cambridge University Press